Optimizing Spatial Planning of Small-scale Green Infrastructure to Mitigate Urban Heat Islands in Hong Kong

Hoi Nam Hellas Lee

ABSTRACT

With rising surface temperatures due to climate change, especially in urban areas, regulators have turned to green infrastructure (GI) to effectively adapt to urban heat islands (UHIs) and increase climate resilience. Small-scale implementation is of particular focus in Hong Kong due to limited land space, but the extent to which they effectively mitigate urban heat is highly dependent on their physical characteristics and spatial connectivity. This study evaluates the current GI network's ability to mitigate UHIs in two Hong Kong districts: Tuen Mun and Yau Tsim Mong, finding that the vegetation configurations between the two districts vary substantially, hence affecting the range of land surface temperature (LST), hotspots, and coldspots observed. Characterizing the GI based on the following landscape network metrics: vegetation percentage, perimeter-area ratio, vegetation area, nearest neighbor distance, and largest patch dominance, I analyzed their relationships with (LST) in hotspots and coldspots in the study areas. From my correlation analysis, I identified perimeter-area ratio and vegetation percentage to be major metrics of consideration for the future planning of GI to address UHIs. However, the large variability in correlation strengths between the two districts, hotspots, and coldspots highlights the need for careful evaluations in ensuring that GI networks contribute to reducing UHIs in Hong Kong.

KEYWORDS

landscape network metrics, street-level greenery, geospatial analysis, hotspot analysis, linear regression

INTRODUCTION

Climate change impacts are of increasing concern, leading to a movement within environmental policy and planning to determine how our societies can adapt and become resilient to them. Such developments are often seen on the city scale, where the majority of the human population resides, with a projected rise to 80% of the world's population living in urban settings by 2050 (Venditti 2022). Additionally, cities account for over 70% of greenhouse gas emissions, with the World Bank recognizing city systems as one with the greatest emissions and significant adaptation challenges (Dasgupta et al. 2022). Within environmental policy guidelines, climate mitigation strategies have been the predominant focus, as society aims to reduce greenhouse gas emissions to reduce further warming. However, the latest IPCC 6th Assessment Report (AR6) states that with near-term global warming expected to reach 1.5°C, climate-related extreme events and limitations on resource availability will be pressing issues. This is particularly in cities, where temperatures are on average 1-3°C warmer than their surroundings. Compounded with high population densities and material consumption, these currently observed impacts and projected risks demonstrate the urgency we must operate under for climate-resilient development action (IPCC 2022, Zielinski 2014). This has led to a paradigm shift in sustainable environmental planning to one establishing adaptation and resilience strategies so societies can adapt to extreme weather events and other climate impacts (Hill 2016).

One such impact is urban heat islands (UHIs) and heatwaves. Heatwaves are periods of hot weather lasting for days, with their effects often exacerbated in cities (World Health Organization n.d.). UHI refers to instances of relatively higher atmospheric and surface temperatures in urban areas compared to their surroundings, such as a neighboring rural area, or in intra-urban heat island (IUHI) analysis, cooler areas within city limits (Maimaitiyiming et al. 2014, Bruns and Simko 2017). This phenomenon is common among big cities worldwide, with over 90% showing evidence of surface UHIs (Peng et al. 2012). As such, global exposure has grown 199% over approximately 30 years, with 34% attributed to urban warming, affecting 1.7 billion people in 2016 (Tuholske et al. 2021). Future heatwaves are likely to become more frequent, more severe, and last longer. An absolute heatwave temperature increase of 3.4-6.6°C between 2066 and 2099 is projected in populous cities and over 99% of children will experience at least 4.5 heatwaves annually by 2050 under high-emissions scenarios (Brown 2020, United

Nations Children's Fund 2022). Adaptation and resilience towards intensifying urban warming is necessary for urban areas as they continue to develop, ideally through multifunctional approaches.

Urban GI, which this investigation defines as the planned application of vegetation in an urban area, such as parks and rooftop gardens, has been presented as a promising, multifunctional strategy to address both climate adaptation and mitigation goals. There is a wide variety of small-scale GI including, rain gardens, rooftop gardens, parklets, pocket forests, and bioswales (Razzaghi Asl and Pearsall 2022). These forms of GI contribute significantly to cooling in an urban context, especially where land use may be contentious, making them imperative in future environmental planning. Theoretically, they can address several climate impacts, such as reducing flood risk, improving water quality, and reducing UHIs (Kim and Song 2019, Parker and Zingoni de Baro 2019, Sturiale and Scuderi 2019, Choi et al. 2021). Their benefits within an urban context make GI an important environmental planning tool for economic, social and environmental development.

However, in practice, the effectiveness of GI in addressing these goals is highly dependent on its location, size, and landscape characteristics (e.g., Bowler et al. 2010, Kong et al. 2014), and hence, on land use planning. In planning GI, reducing the UHI effect is not often the primary goal, if even considered. For example, the Mirabeau Garden in New Orleans was designed as part of the Gentilly Resilience District to reduce flood and subsidence risk while educating about stormwater management (City of New Orleans 2019). Although mitigating urban heat was listed as a benefit in late 2019, the project objectives in 2018 did not include urban heat considerations (City of New Orleans 2018). As a result, there is often an unequal distribution of GI and UHI within a city, and the placement of GI may even be exacerbating UHI inequities. Small-scale GI has the potential to improve the interconnectivity between existing sites, making them a beneficial mechanism to deliver a more equal distribution of surface temperature across the local community (Jerome 2017). As such, a larger-scale landscape network scale may be beneficial to determine the relationship between GI and their collective benefits in reducing UHI. Such network analysis will determine the optimal applications of GI for a wider cooling effect to build a city's overall resilience toward urban heat.

This study generates a deeper understanding of the most effective and optimal applications of small-scale GI in addressing climate adaptation goals to reduce UHIs in Hong

Kong. The city acts as a useful area to study due to its densely built environment and relatively high summer temperatures. To address this, I evaluated the extent to which the current GI contributes to thermal hotspots and coldspots to present a baseline scenario and identify current hotspots across the landscape. I expected an unequal distribution of GI and UHIs to emerge and hence identify areas where future implementation of GI would be beneficial. From there, a comparison of different characteristics defining GI's physical dimensions is presented to determine the criteria for optimal effectiveness in reducing hotspots, with a particular focus on vegetation area and perimeter-area ratio. Lastly, I used network analysis to provide insights into how small-scale GI connectivity can deliver an optimal cooling effect in Hong Kong.

BACKGROUND

Small-scale green infrastructure

Current greening projects and literature evaluating GI often focus on large, singular case studies, rather than small-scale GI. Urban parks and gardens are especially common, although other ground vegetation and green roofs are also popular topics (Bowler et al. 2010, Dronova et al. 2018, Anderson and Gough 2022). Challenges associated with evaluating small-scale GI revolve around the spatial imagery resolution for remote sensing methods and consideration of confounding variables when conducting field experiments. As previous literature has deduced, the cooling benefits associated with a small area of GI by itself are also less significant on a wider spatial scale compared to larger forms of GI (Kong et al. 2014, Vaz Monteiro et al. 2016, Du et al. 2017, Masoudi and Tan 2019).

However, as land use becomes increasingly contentious, especially in dense cities such as Hong Kong, it is imperative that small-scale applications are equally considered in an urban setting. Several studies have investigated small-scale GI in urban areas. Park et al. (2017) investigated the role of small-scale street greenery on air temperature on the urban block scale. The small green spaces are categorized by form (polygonal or linear) and by vegetation characteristics (single or mixed). Then, the area and volume were calculated to determine which factors affected their air temperature measurements. Linear regression models between temperature reduction and area/volume found statistically significant relationships for polygonal

and mixed street greenery. Lin et al. (2017) studied pocket parks in Hong Kong, focusing on a small section of Hong Kong Island. Apart from greenery indicators like tree and shrub areas, Lin et al. included urban design indicators to characterize the local landscape, such as building density, park area, and floor area ratio (FAR). Interestingly, they found a negative correlation between FAR and building density with daytime UHI, which differs from other studies such as Petralli et al. (2014) and Perini & Magliocco (2014), but other correlations and values for cooling intensity were similar.

Landscape network analysis

Due to their limited cooling effects individually, landscape network analysis of small-scale GI is necessary to evaluate its full potential. Interpreting GI interconnectivity and its contribution to larger ecological networks have been an area of focus (Jerome 2017). An analysis using landscape metrics is common among these studies to determine the relationships between GI characteristics and its cooling effect (Table 1). There is a wide range of possible indicators, with the most common being green space area and patch density. Other metrics, such as the percentage of vegetation area and aggregation indexes, were also utilized often, but many were only used in one of the papers listed. Metrics exploring the network connectivity between green spaces were especially sparse, seen only in Masoudi and Tan (2019).

Table 1. Summary of landscape metrics indicators to characterize green infrastructure in literature.

Landscape metric	(Maimaitiyiming et al. 2014)	(Du et al. 2017)	(Masoudi and Tan 2019)	(Vaz Monteiro et al. 2016)	(Kong et al. 2014)	(Jaganmohan et al. 2016)
Green space physical dimensions						
Green space area		●		●		●
Patch density	●		●		●	
Edge density	●		●			
Landscape shape index		●	●			
Mean patch size			●		●	
Number of patches			●			
Area-weighted mean patch size			●			
Area-weighted mean shape index			●			
Mean span				●		
Perimeter-area ratio				●		
Mean patch radius of gyration of forest vegetation					●	
Mean shape index						●
Land use classification						
Percentage of landscape of green space	●		●			
Area/percentage of vegetation		●			●	

Tree/shrub canopy cover				●		●
Grass cover				●		
Vegetation class area			●			
Area/percentage of impervious surfaces		●			●	
Area/percentage of water bodies		●			●	●
Land use diversity					●	
Patch richness of land use					●	
Connectivity of green spaces						
Aggregation index			●		●	
Area-weighted Euclidean nearest neighbour distance			●			
Area-weighted fractal dimension index			●			
Largest patch index			●			
Mean Euclidean nearest neighbour distance			●			
Other metrics						
Distance to city centre						●
Average wind speed						●

From this review, I identified five landscape metrics to characterize small-scale GI beyond their typology, capturing GI physical dimensions and the connectivity of GI:

- Greenspace vegetation area (a larger area is expected to contribute more cooling, holding other factors constant)
- Perimeter-area ratio (smaller values of perimeter-area ratios is expected to contribute more cooling, holding other factors constant)
- Greenspace vegetation percentage (larger percentages of vegetation compared to landscape area are expected to contribute more cooling, holding other factors constant)
- Nearest neighbor distance (smaller values of nearest neighbor distance is expected to contribute more cooling, holding other factors constant)
- Largest patch dominance (larger values of largest patch dominance is expected to contribute more cooling, holding other factors constant)

Study Areas

Hong Kong, located on the coast of southeast China in the tropics, is known for its skyscrapers and bustling city core. The city is projected to see an average temperature rise of 1.1-1.7°C by 2060 and 1.2-3.6°C by 2100 (Hong Kong Observatory 2021).

As such, the local government has outlined several initiatives to reduce UHI impacts. These include sending public alerts for hot weather, providing temporary night heat shelters, and placing more water fountains in public areas (The Legislative Council Commission 2021). In relation to the built environment, the government has taken the lead by incorporating greenery in all public works projects. All government buildings are required to include greenery elements and aim for a Building Environmental Assessment Method (BEAM) Plus certification, the local criteria for assessing building sustainability (BEAM Society Limited n.d.). To incentivize new private buildings to include green features, gross floor area concessions are applicable to developers as long as they are registered under BEAM Plus. In the city's 2050 climate action plan, the government outlines that the continuous enhancement of policies to review design standards and the concession's granting mechanism are actions in upcoming years to ensure effective UHI mitigation in the city (Hong Kong SAR Government 2021).

Actions addressing UHIs are particularly important in the urban built environment of Hong Kong, with complexities related to its heterogeneous landscape. Up to 40% of the city's land area is public green space, but the majority consists of large country parks, green belts, and conservation areas (Lai 2017). Most residential and commercial activity exists on 25% of the total available land (Lee 2020). Instead, the government's Planning Department outlines countable open space (COS) in the urban cores, which are usually small recreational spaces embedded within the built environment. Hong Kong Planning Standards and Guidelines outline a minimum of 2 m^2 of COS per person in urban areas and new towns, and 0.5 m^2 per worker in commercial and industrial areas (Lai 2017). While all districts satisfy these requirements, a study by Hong Kong's Civic Exchange demonstrates how open space area varies considerably between the 18 different districts of Hong Kong, from 2.1 m^2 per person to 6.0 m^2 per person. This suggests that studies into GI and greenery should be conducted at a district level.

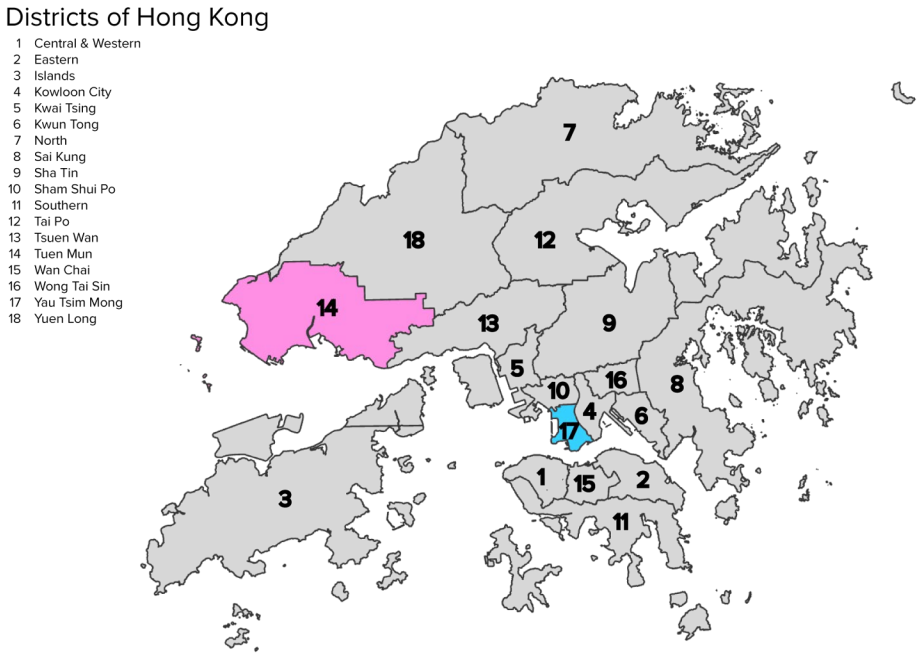

Figure 1. Hong Kong Districts Map.

Tuen Mun (pink) and Yau Tsim Mong (blue) are highlighted. Adapted from Environmental Systems Research Institute (ESRI) Hong Kong.

Yau Tsim Mong district, which consists of the Yau Ma Tei, Tsim Sha Tsui, and Mong Kok regions, is part of the Kowloon Peninsula urban core, adjacent to Victoria Harbour (ESRI

Hong Kong 2022). With the third-highest district population density at 44,460 people per km^2, the region is heavily dominated by both residential and commercial activities, with major retail and financial centers (Yau Tsim Mong District Council 2015, Census and Statistics Department n.d.). Hong Kong climate averages are determined based on the values recorded at Hong Kong Observatory, which is located in this district. Mean temperatures are between 16.5°C and 28.9°C, with January and July typically being the coldest and warmest months respectively (Hong Kong Observatory 2021). The two areas of Yau Ma Tei and Mong Kok are key in Hong Kong's urban redevelopment efforts as their high volume of aging building stock and urban decay are outpacing the current rate of redevelopment and rehabilitation. There have recently been many projects within the district, but the Urban Renewal Authority conducted a study in 2017 noting that a holistic, district-based approach is necessary to deal with urban decay (Urban Renewal Authority n.d.). With such change, there is great potential for the implementation of GI along with urban renewal, especially on a small scale.

Tuen Mun district, situated in the west, away from the urban core (Figure 1), was established in the 1970s. Relative to the mean temperature recorded at the Hong Kong Observatory, Tuen Mun shows a slightly greater temperature range, with values about 0.5°C higher in the summer and about 0.2°C lower in the winter (Hong Kong Observatory 2021). It is known as a first-generation New Town, which was developed as part of a decentralization strategy for urban development away from congested urban areas (Tuen Mun and Yuen Long West District Planning Office, Planning Department 2019). Planning of the New Town revolved around concepts of "balanced development" and "self-containment", resulting in a multi-functional and heterogeneous landscape (Tuen Mun and Yuen Long West District Planning Office, Planning Department 2019). There is a great contrast between the goals of planning with New Towns in comparison to the urban areas of Yau Tsim Mong district, so understanding the role of small-scale GI in both urban landscapes is important for the future sustainable development across Hong Kong.

METHODS

Calculating land surface temperature (LST)

Satellite imagery from the United States Geological Survey (USGS) was downloaded through EarthExplorer (https://earthexplorer.usgs.gov/). The criteria for choosing the imagery date was first based on location availability. Specifically, the imagery had to include both Tuen Mun and Yau Tsim Mong. In order to capture the effects of UHIs during the summer months, which is when urban heat is of particular concern, I narrowed my date range to between June 1st, 2022, and August 31st, 2022. From there, imagery with little cloud cover was preferred, as well as images during periods of relatively higher summer temperatures. With this criteria, imagery from 25th July 2022 was taken from Landsat 9 Collection-2 Level-1.

The following equations were used to calculate land surface temperatures (LST) from Bands 4, 5, and 10 of the downloaded imagery (*Estimating the Land Surface Temperature (LST) using Landsat 8 in ArcGIS* 2021). These bands correspond to the red spectrum (wavelengths: 0.64 - 0.67 µm), near-infrared (wavelengths: 0.85 - 0.88 µm), and thermal infrared (wavelengths: 10.6 - 11.19 µm) respectively (U.S. Geological Survey n.d.).

$$Top\ of\ Atmosphere\ (TOA)\ Total\ Spectral\ Radiance\ =\ ML\ \times Q_{cal} \times AL \times Q_{i} \quad \text{(Eq. 1)}$$

$$where\ ML = 3.342 \times 10^{-4},\ Q_{cal} = Band\ 10\ radiance,\ AL\ =\ 0.1,\ and\ Q_{i} =\ -0.29$$

$$Brightness\ Temperature\ (BT)(°C)\ =\ \frac{K_2}{[ln(\frac{K_1}{TOA})+1]} - 273.15 \quad \text{(Eq. 2)}$$

$$where\ K_2 =\ 1321.0789\ and\ K_1 =\ 774.8853$$

$$NDVI \quad \frac{Band\ 5 - Band\ 4}{Band\ 5 + Band\ 4} \quad \text{(Eq. 3)}$$

$$Proportion\ of\ vegetation\ (Pv)\ = (\frac{NDVI - NDVI_{min}}{NDVI_{max} - NDVI_{min}})^2 \quad \text{(Eq. 4)}$$

$$Land\ surface\ emissivity\ (\varepsilon)\ =\ 0.004Pv + 0.986 \quad \text{(Eq. 5)}$$

$$Land\ surface\ temperature\ (LST)\ =\ \frac{BT}{1+(\frac{10.895BT}{1438})\times ln(\varepsilon)} \quad \text{(Eq. 6)}$$

Determining areas for analysis

With the LST maps produced, I chose to analyze the differences between the hotspots and the coldspots in each district. As the calculated LST distribution represented a normal distribution, with little skew, I determined that a percentile cutoff was appropriate for defining the areas for analysis. First, the top 20% and bottom 20% of the LST range were isolated for hotspots and coldspots respectively. Then, the top 10% and bottom 10% of the LST range were also isolated. Areas isolated with the 20th percentile cutoff that also had temperatures in the upper and lower 10th percentiles were chosen as the final hotspots and coldspots, respectively, for analysis.

Analysis of current vegetation network and impact on LST

High-resolution satellite imagery from PlanetLabs data was used to ensure small-scale GI could be captured in the vegetation mapping process. With a pixel resolution of 3 meters x 3 meters, an image from the 25th July 2022 was used to match that of the Landsat 9 imagery.

To classify the land uses into four general categories: vegetation, developed built environment, water, and clouds, I used both the supervised and unsupervised classification wizard programs on ArcGIS Pro. From there, I isolated the vegetation layer and clipped them to visualize the vegetation network in each hotspot and coldspot.

For each analysis area, the parameters needed for each landscape network metric were calculated through ArcGIS Pro. This included vegetation perimeter, vegetation area, nearest neighbor distance, and hotspot or coldspot area. Table 2 lists the chosen landscape network metrics and their calculations from these parameters.

Table 2: Calculation of landscape network metrics

Landscape Network Metric	**Calculation from parameters**
Vegetation area	Vegetation area as provided by ArcGIS Pro
Vegetation perimeter-area ratio	$\frac{Vegetation\ Perimeter}{Vegetation\ Area}$
Vegetation percentage	$\frac{Vegetation\ area}{Hotspot/Coldspot\ area}$
Nearest neighbor distance	Nearest neighbor distance as provided by ArcGIS Pro
Largest patch dominance	$\frac{Vegetation\ area\ [Largest\ patch]}{Hotspot/Coldspot\ area}$

With the calculated landscape network metrics, single linear regression analysis was conducted to determine the correlations between the vegetation characteristics and the mean LST in each hotspot or coldspot. The analyzed data points representing hotspots or coldspots were grouped in various ways. First, my analysis was for both hotspots and coldspots in each district to determine the district-scale trends and compare the regional differences in correlation. Then, regression analysis for all the hotspots and all the coldspots in both districts was also conducted to differentiate trends that would contribute to creating hotter and colder environments respectively.

Following the single variable linear regression analysis, a multiple variable linear regression for the four groups (Tuen Mun, Yau Tsim Mong, all hotspots, and all coldspots) was also conducted to figure out how the combination of such metrics could contribute to the LST patterns.

However, further analysis had to be done for the multiple variable linear regression upon finding that some of the landscape network metrics had very strong correlations with each other, especially for the data analysis for each district. Thus, their combined influence on LST may result in an inaccurate model. As such, from the calculated correlation matrix, if there were variables that were strongly correlated ($|R^2| > 0.60$) with each other, only one was chosen to be integrated into the linear regression analysis. A refined model to determine LST was derived from there. The results of this analysis then informed which metrics should be considered in the planning of GI in both districts and the extent to which they affect LST hotspots and coldspots.

RESULTS

Relationship between current green infrastructure and land surface temperature

Land surface temperature distribution

The land surface temperature range in the two districts did not vary too substantially. In Tuen Mun, the temperatures ranged from 21.75°C to 40.60°C, while in Yau Tsim Mong, the calculated LST was 26.72°C to 38.43°C (Fig. 2). Tuen Mun exhibited a greater range of temperatures, although the means of the temperature distribution were only about 1°C apart. The temperature distributions are relatively representative of a normal distribution, with little skew. Hotspots and coldspots in Tuen Mun are above 33.80 and below 26.70 respectively, while the boundaries for these extremes in Yau Tsim Mong are 33.42°C and 26.72°C respectively. The spatial distribution of temperature was uneven in both districts. In particular, areas of lower temperatures in Tuen Mun were in the mountainous and forested areas while in Yau Tsim Mong, these cooler areas were along the coastline. Areas of densely built environments in both locations had relatively higher LST. There were also patches of hotspots and coldspots that were directly adjacent to each other or overlapping in Yau Tsim Mong, which is an interesting observation. There are 19 major patches for further investigation (Fig. 3).

Figure 2: Histogram of LST distribution for Tuen Mun (top) and Yau Tsim Mong (bottom)

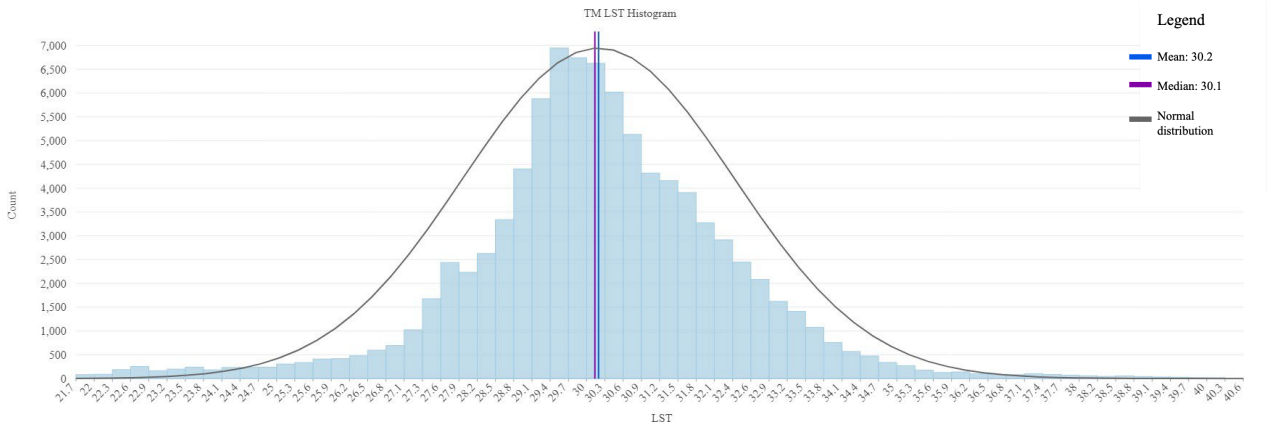

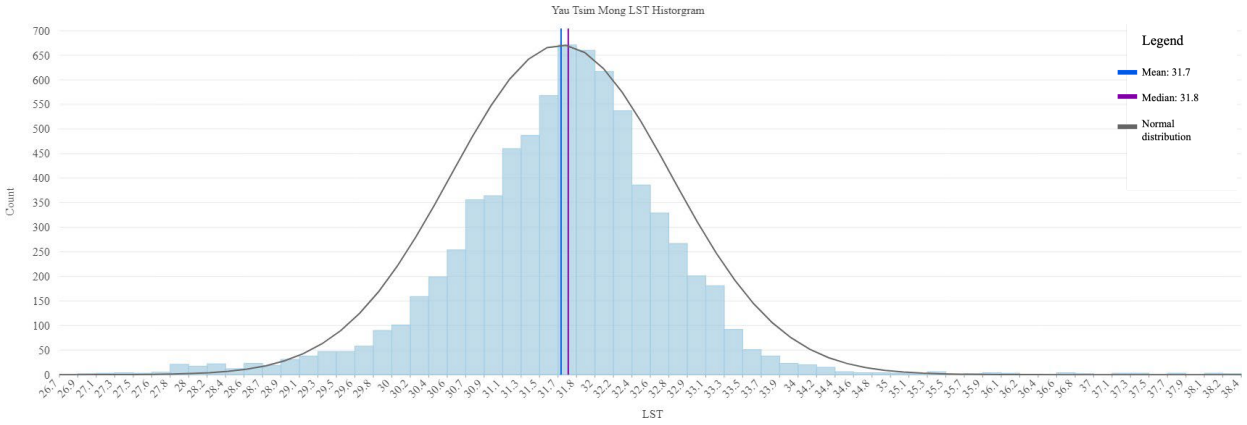

Figure 3: Hotspots (red) and coldspots (blue) and the derived vegetation network (green) in Tuen Mun (top) and Yau Tsim Mong (bottom)

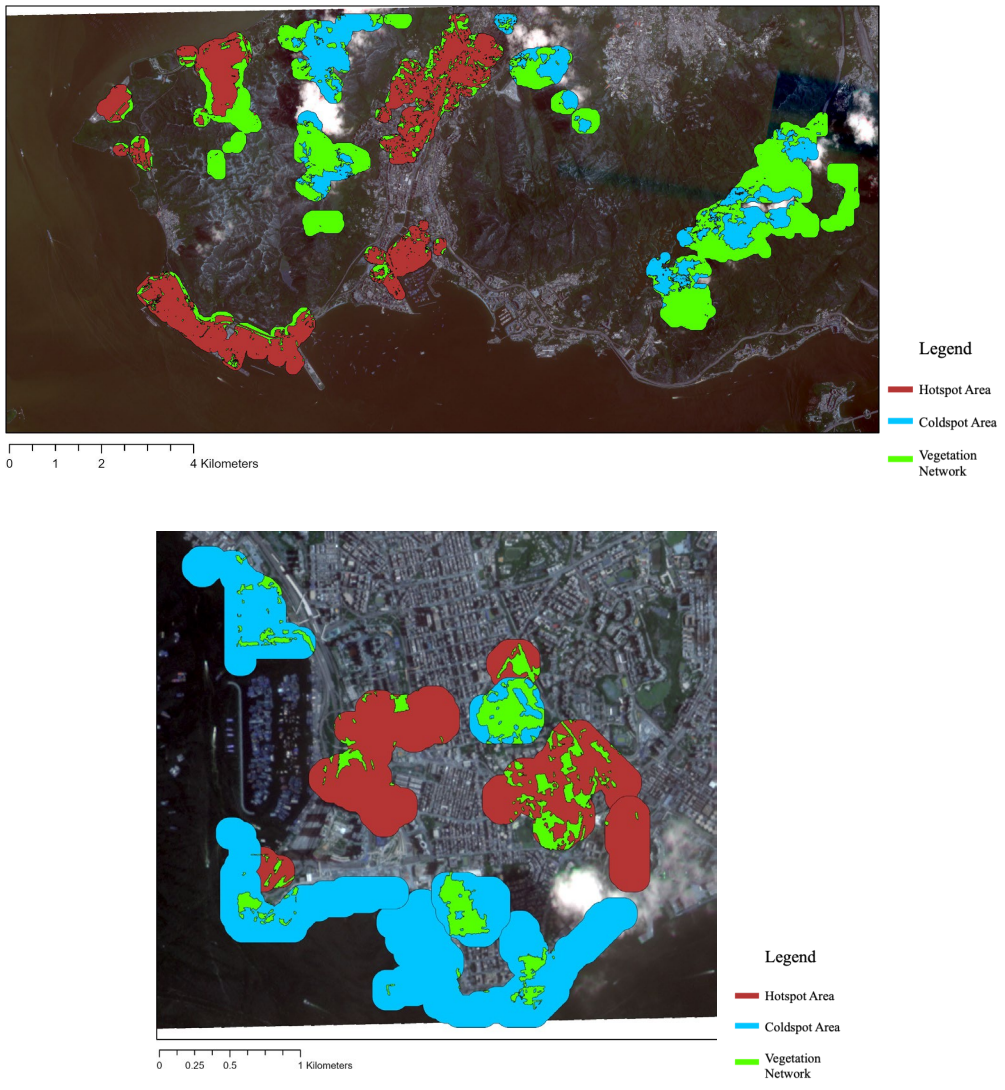

Current green infrastructure/vegetation distribution

Vegetation in Tuen Mun is highly dominated by mountainous and forested areas, with a considerable difference in vegetation cover and size between the hotspots and the coldspots. The hotspots in Tuen Mun have more vegetation of smaller size and greater fragmentation, with the exception of TM_Hot_2, which has a large patch of vegetation towards the South (Fig. 4). On the other hand, vegetation in Yau Tsim Mong appears to be relatively similar between the hotspots and the coldspots. Compared to Tuen Mun, the vegetation patches are smaller in size, attributed mostly to the smaller hotspot/coldspot areas.

Figure 4: Hotspots and Coldspots for both districts

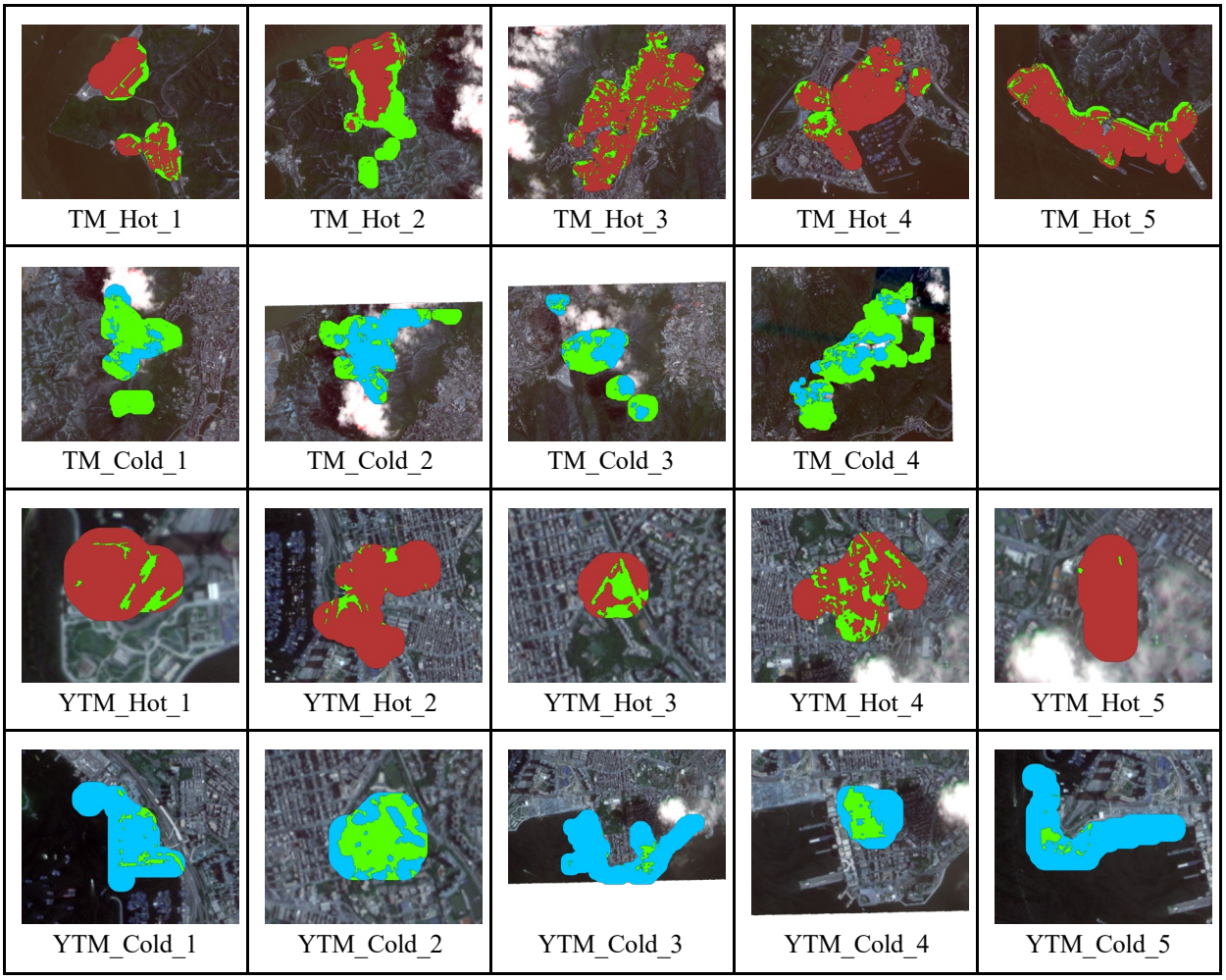

Correlation between landscape network metrics and land surface temperature

The three landscape network metrics to evaluate GI physical characteristics are vegetation percentage, perimeter-area ratio, and vegetation area. Nearest neighbor distance and largest patch dominance are used as metrics to evaluate green infrastructure connectivity. Through the single linear regression analysis, only 5 of the 20 relationships yielded statistically significant (p-value < 0.005) results (Table 3). For Tuen Mun, this is for vegetation percentage, which resulted in a negative correlation. No significant relationships were found for Yau Tsim Mong. The analysis of hotspots showed a positive correlation between LST and the metrics of vegetation percentage, vegetation area, and largest patch dominance. Lastly, coldspots LST was significantly correlated with the perimeter-area ratio.

Table 3: Single linear regression R^2 values for landscape network metrics.

	Vegetation Percentage	Vegetation Area	Perimeter Area Ratio	Nearest Neighbour Distance	Largest Patch Dominance
Tuen Mun	**0.486**	0.187	0.154	0.203	0.160
Yau Tsim Mong	0.006	0.086	0.010	0.033	0.030
Hotspots	**0.588**	**0.669**	0.109	0.085	**0.573**
Coldspots	0.421	0.00005	**0.750**	0.050	0.141

Cells in green represent positive correlations, while red cells indicate negative correlations. Values in bold are statistically significant correlations.

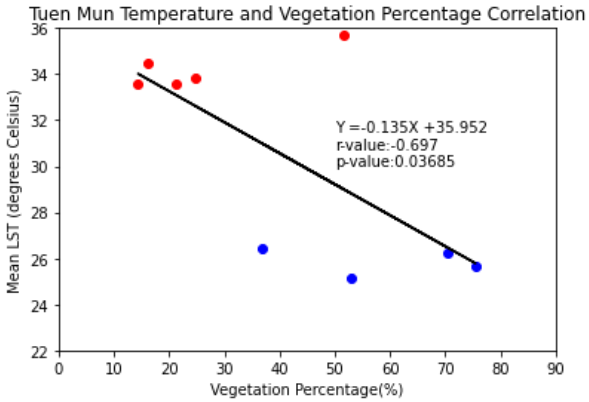

Figure 5a: Tuen Mun LST and Vegetation Percentage Correlation

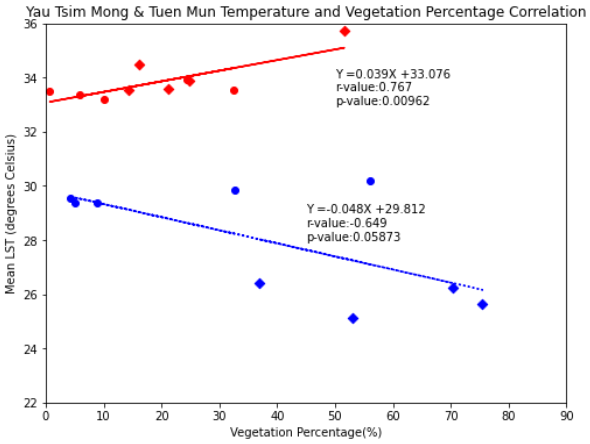

Figure 5b: Hotspot and Coldspot LST and Vegetation Percentage Correlation

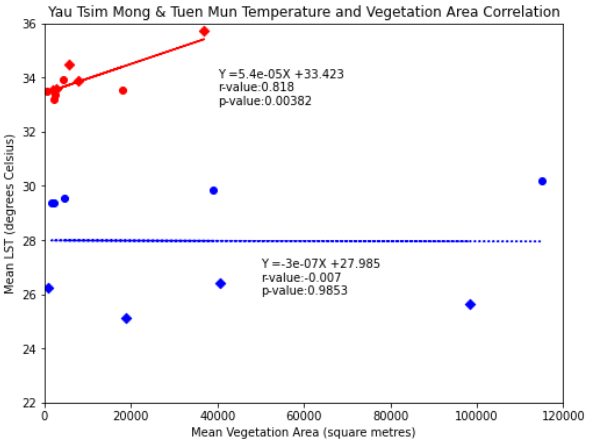

Figure 5c: Hotspot and Coldspots LST and Vegetation Area Correlation

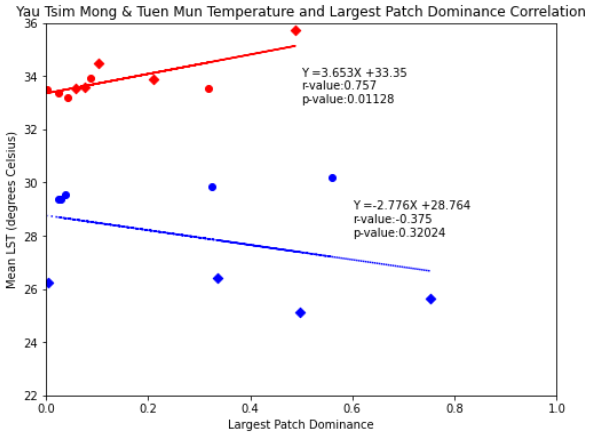

Figure 5d: Hotspot and Coldspot LST and Largest Patch Dominance Correlation

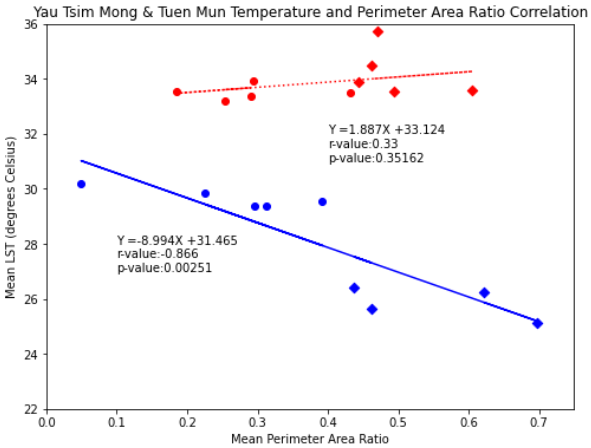

Figure 5e: Hotspot and Coldspot LST and Perimeter Area Ratio Correlation

From the preliminary multiple variable linear regression analysis, not accounting for correlation between metrics, only the one conducted on the coldspots resulted in a statistically significant relationship, with an R^2 value of 0.989. From the analysis, 4 of the 5 metrics were statistically significant as a regression predictor of LST: vegetation percentage, vegetation area, perimeter-area ratio, and nearest neighbor distance (Table 4).

Table 4: Statistical significance of landscape network metrics in preliminary coldspot multiple linear regression analysis with LST as a dependent variable

Landscape network metric	P > |t|	Regression coefficient	Regression coefficient (normalized values)
Vegetation percentage	0.066	0.0529	0.7095
Vegetation area	0.040	-18.6436	-1.5045
Perimeter-area ratio	0.007	-7.147×10^{-5}	-1.7961
Nearest neighbor distance	0.036	0.0268	0.4308
Largest patch dominance	0.121	4.2233	0.5704

With the refined linear regression, for Tuen Mun, the metrics were vegetation percentage, perimeter-area ratio, and vegetation area. The metrics for Yau Tsim Mong were nearest neighbor distance and vegetation area. Both regressions still did not yield an F-statistic of below 0.05, and none of the metrics were deemed statistically significant regression predictors for LST. For the coldspots, the refined multiple linear regression removed vegetation area as an independent variable. The resulting regression had an R^2 value of 0.945, but apart from the perimeter-area ratio, none of the other metrics were statistically significant regression predictors (Table 5).

Table 5: Statistical significance of landscape network metrics in refined coldspot multiple linear regression analysis with LST as a dependent variable

Landscape network metric	P > |t|	Regression coefficient	Regression coefficient (normalized values)
Vegetation percentage	0.765	-0.0052	-0.0699
Perimeter-area ratio	0.004	-9.0534	-0.8722
Nearest neighbor distance	0.452	0.0084	0.1355
Largest patch dominance	0.145	-2.2564	-0.3047

DISCUSSION

The results of the correlation analysis help inform planning management strategies for each district specifically, and for how hotspots can be managed through GI in Hong Kong more generally. The correlation between the analyzed landscape network metrics and the mean LST of the hotspot or coldspot varies depending on how the data is grouped, highlighting how the effects of GI physical characteristics and connectivity are a very local phenomenon. Despite this, perimeter-area ratio and vegetation percentage, the latter of which is applicable for Tuen Mun, should be more heavily considered in GI planning and management to reduce UHIs observed within the urban landscape.

The effects of vegetation configuration on land surface temperature for each district

Based on the calculated areas of vegetation and the patterns of land surface temperature, the ability of the current GI networks to mitigate UHI varies between the two districts. In Tuen Mun, there are significant differences in vegetation configuration between the hotspots and the coldspots. With the hotspots generally having smaller, fragmented vegetation patches, it is suggested that vegetation presence contributes to the larger temperature range observed (Fig. 2). The exception to this observation, TM_Hot_2, can be explained by the presence of a major landfill, which emits fossil fuels. The highly localized emission of methane contributes to the high LST values observed, which the nearby vegetation cannot mitigate.

These general observations are reflected in the correlation between vegetation area and mean LST. As such, in Tuen Mun, vegetation percentage is a greater factor in determining UHI mitigation with GI, without regard for vegetation size or its connectivity. While the correlation strengths of the other metrics were insignificant and weak, the direction of the relationship was as expected, with the exception of largest patch dominance. The negative relationship suggests further support for the use of small-scale GI to reach a threshold of vegetation proportion, rather than having a singular, large-scale GI.

On the other hand, there are few discernible differences in the vegetation patches in Yau Tsim Mong. Both the identified coldspots and hotspots have similar small fragments of vegetation, except for YTM_Cold_2, YTM_Cold_4, and YTM_Hot_3. The presence of the remaining coldspots may be attributed to the surrounding water bodies, as they are all along the coastline. As such, planning GI in Yau Tsim Mong will also need to consider proximity to water bodies when determining how much greenery is necessary to reduce UHI. This is important, especially considering that none of the landscape network metrics showed any significant correlation with the mean LST of the analyzed hotspots and coldspots.

Based on the insignificant linear regression results, both in the preliminary stages and after refining to account for strong metric correlations, it is difficult to discern how the combination of landscape network metrics should shape GI planning on the district scale.

Implications for district planning management

These observations reflect the different planning management of the two districts. The topographical restrictions present in Tuen Mun result in a large contrast despite the original goals of balanced development. The district greatly relies on the presence of surrounding natural areas to mitigate UHIs. In Yau Tsim Mong, the flat, urban land throughout the whole district necessitates the presence of GI throughout urban development initiatives to reduce UHI if the land parcels are not by the water. As such, the distribution of green spaces is relatively uniform between the hotspots and coldspots, although in absolute area size, there is substantially less greenery than there is in Tuen Mun. Even with new urban redevelopment initiatives, the infrastructure lock-in may still result in similar land use patterns in Yau Tsim Mong. From the results determining the correlation between the landscape network metrics and LST in the

extreme temperature spots, we can see that the selected landscape network metrics alone cannot account for all the variability in LST distribution on the district scale.

The effects of vegetation configuration on hotspots and coldspots

Looking at the correlations that are significant for the hotspots across both districts, some interesting observations emerge. Vegetation percentage, vegetation area, and largest patch dominance all present with strong positive correlations with mean LST, implying that increasing the proportion and size of GI for a given area may further exacerbate the presence of UHI. This means that other factors may be hindering the realization of GI cooling effects, and other considerations may be necessary to reduce these hotspots. These may include considerations about building floor-area ratios or how the built environment may reduce the ventilation of air. Lan et al. used ENVI-met micro-scale simulations to determine how building configuration, ventilation and greenery may affect urban heat islands and thermal comfort. Their results showed that apart from adding greenery, the existing building configuration could be further improved by adding a singular high-rise building and having ventilation corridors (Lan et al. 2021). Ng et al. also conducted an earlier study on Yau Tsim Mong are found a significant difference in greenery recommendations when buildings are below 20 meters versus when they are above 40 meters high, especially in the effectiveness of rooftop gardens in mitigating urban heat islands. Sky-view factor and wind paths may also be a consideration in landscape management (Tan et al. 2016) Particularly in a complex urban landscape, these built environment factors may contribute more significantly to thermal distribution and are confounding variables to consider in GI landscape analysis.

Despite the challenges presented by the hotspot correlations, the insights from the coldspot linear regressions do provide a direction for factors to consider to create these coldspots. Perimeter-area ratio and mean LST has the strongest correlation out of the single variable linear regressions conducted. The negative relationship suggests that higher GI with higher perimeter-area ratios would be more effective in generating a surrounding cooling effect. With a fixed area, triangles and squares are shapes that increase the perimeter-area ratio, but adding complexity to the shape to increase the GI's edge effects also results in the desired effect.

In addition, the multiple variable linear regression provides support for a suite of landscape network metrics to be considered in GI planning to create coldspots. With the refined regression analysis, the direction of the correlation between the metrics and LST was as expected, with the exception of perimeter-area ratio, where a negative correlation was observed. This is in contrast to the findings from Vaz Monteiro et al. and Kong et al., where higher perimeter-area ratios were found to reduce the amount of cooling, both in intensity and spatial distance. This is particularly interesting due to the strong correlation observed in the single linear regression analysis for coldspots and with this metric being the only statistically significant regression predictor in this analysis.

Based on the collective observations from my correlation analysis, my recommendation is for perimeter-area ratio to be heavily considered in the design of GI interventions to mitigate UHI. In Tuen Mun, vegetation percentage should also be taken into heavy consideration. These recommendations for landscape network metrics have some alignment with those from other studies. Masoudi and Tan's analysis of Singapore's green infrastructure found that the percentage of landscape, area-weighted mean shape index, patch density, and area-weighted Euclidean nearest neighbor distance were the four metrics that adequately characterized LST. Area-weighted perimeter-area ratio is noted to be a significant metric for Kong et al., where they also observed a strong correlation, although they observed a positive relationship between the two variables.

With these two metrics in mind, planning small-scale GI in both of these districts will require careful insight into both GI physical characteristics, both on the wider landscape scale with vegetation percentage, and on the patch scale with perimeter-area ratio. However, connectivity GI in both of these districts is not necessarily a priority consideration. Similar districts in Hong Kong, such as other New Territory districts and those along the Kowloon Peninsula, may also benefit from these observations. In addressing these considerations through a regulatory approach, districts in Hong Kong can effectively plan GI to reduce these observed hotspots and mitigate the impacts of UHIs.

Limitations and future directions

Although this study gathers some conclusions about the planning considerations to effectively reduce UHIs, these have limitations and warrant future research. In particular, this study only captures one daytime instance of LST during the summer of 2022. To gain a better idea of how GI contributes to LST in both districts, using more satellite imagery and comparing diurnal trends would be useful for more holistic planning proposals. In addition, using the classification wizard in ArcGIS Pro, even with high-resolution imagery, may yield some errors in the vegetation mapping, especially since I did not correct for the presence of clouds in the classification process. As such, there may be instances where the derived vegetation network does not match the actual network present in both districts. Lastly, while a buffer region of 100 meters was considered in the vegetation analysis, there were some large-scale GI, especially in Tuen Mun, which were clipped in this analysis. Hence, the effects of a whole forested area were assumed to be that of the clipped section of it, which may not be accurate in its effects on LST.

In relation to the correlation analysis, there were limitations in the conclusions I could make due to the small sample sizes in each of the groups. The use of hotspots and coldspots to characterize whole districts led to a more discrete perspective of the landscape, which may have contributed to the lack of significant correlations in both the single and multiple-variable linear regression analysis. With more data, either with more hotspots and coldspots or with more districts for a more general perspective, a more accurate model could be created to make more concrete conclusions about how landscape network metrics could alleviate thermal hotspots and reduce LST where necessary.

In addition, mitigating UHIs is only one of the benefits that GI brings to a community, both on the macro and micro-scale. The results of this investigation should not be the exclusive source of planning recommendations. A more integrated and proactive approach that encompasses all the ecological services that GI can provide is a necessary shift in planning approaches (Lennon and Scott 2014). An example of such an approach in planning GI is the Green Infrastructure Spatial Planning model created by Meerow and Newell. They integrate six benefits of GI, encompassing both social and ecological resilience goals such as stormwater management and social vulnerability, and apply the model to Detroit to reveal the locations in which such benefits can be maximized (Meerow and Newell 2017). To provide a more holistic

and comprehensive evaluation of GI planning, an assessment considering the multiple benefits of GI would be necessary and would inform planners more directly.

As suggested throughout this study, the observations and recommendations are highly dependent on the particular land use characteristics of the study area. The differing results of the two districts provide an indication of the high specificity of the outlined recommendations, but generalizing their land use characteristics may provide an idea of how other regions may implement GI effectively to mitigate UHI. Other studies have also found limited transferability of their results to other cities, noting that while their framework can be applied, the locale-specific characteristics outweigh the general recommendations when providing effective recommendations (Makido et al. 2019; Marando et al. 2022; Zhou et al. 2017). As such, the results of these studies are most applicable to cities with a similar climate and similar land-use or built environmental characteristics, such as cities in the Greater Bay Area.

CONCLUSION

This study provides a basis for understanding the vegetation configuration and landscape network factors that contribute to alleviating thermal hotspots in Hong Kong. The current GI network in both Tuen Mun and Yau Tsim Mong contributes to the patterns of LST and its inequitable distribution, as shown through the identified hotspots and coldspots. Through a correlation analysis of five landscape network metrics characterizing GI physical dimensions and connectivity, I identified substantial differences in how these metrics were related to LST for the two districts and also found that these correlations differ between the hotspots and the coldspots. Observations from both the single and multiple-variable linear regression models lead to my recommendation of using perimeter-area ratio and vegetation percentage as priority indicators for future GI planning. However, given the wide range of variability observed in this study, it is imperative that there is a more holistic and careful evaluation of GI planning in Hong Kong and beyond. This way, the benefits of GI in reducing UHIs, and perhaps their other co-benefits, can be successfully optimized to create more climate-resilient urban areas.

ACKNOWLEDGEMENTS

This thesis would not have come to fruition without the support of Iryna Dronova, and the ESPM 175 teaching team: Patina Mendez, Robin Lopez, and Danielle Perryman. Thank you all for your time, resources, and support throughout this past year. Navigating a new field of landscape management while learning GIS for the first time would have felt extremely daunting if it were not for your guidance in shaping my project. In particular, I would like to thank Iryna Dronova for taking me on as a mentee and being so enthusiastic about my vision with this thesis. I am so thankful that you decided to take the time to mentor me on top of your other responsibilities - I do not think I would have been able to do this project otherwise.

Thank you to my ESPM 175 working group for your feedback and support throughout this whole process as well. Talking about the different ways we are tackling green infrastructure issues has made me appreciate all the perspectives this topic can be taken, and I am so glad I had the chance to work with all of you this year. In addition, I am so appreciative of the support of my parents, my boyfriend, Sean Fu, and Sarah Zhang. Thank you for listening to me talk about my thesis and for assisting me with my code over this past year. None of this would have been written without your support. Last but not least, if you have made it this far, thank you so much for your time in reading this paper.

REFERENCES

Anderson, V., and W. A. Gough. 2022. Nature-based cooling potential: a multi-type green infrastructure evaluation in Toronto, Ontario, Canada. International Journal of Biometeorology 66:397–410.

Araos, M., L. Berrang-Ford, J. D. Ford, S. E. Austin, R. Biesbroek, and A. Lesnikowski. 2016. Climate change adaptation planning in large cities: A systematic global assessment. Environmental Science & Policy 66:375–382.

BEAM Society Limited. (n.d.). BEAM | Why BEAM Plus. https://www.beamsociety.org.hk/BEAM-Plus/Why-BEAM-Plus.

Bowler, D. E., L. Buyung-Ali, T. M. Knight, and A. S. Pullin. 2010. Urban greening to cool towns and cities: A systematic review of the empirical evidence. Landscape and Urban Planning 97:147–155.

Brown, S. J. 2020. Future changes in heatwave severity, duration and frequency due to climate change for the most populous cities. Weather and Climate Extremes 30:100278.

Bruns, J., and V. Simko. 2017. Stable Hotspot Analysis for Intra-Urban Heat Islands. GI_Forum 1:79–92.

Census and Statistics Department. (n.d.). C&SD : Table E489 : Land area, mid-year population and population density by District Council district. https://www.censtatd.gov.hk/en/EIndexbySubject.html?pcode=D5320189&scode=150&file=D5320189B2021AN21B.xlsx.

Choi, C., P. Berry, and A. Smith. 2021. The climate benefits, co-benefits, and trade-offs of green infrastructure: A systematic literature review. Journal of Environmental Management 291:112583.

City of New Orleans. 2018, March. Mirabeau Water Garden - Fact Sheet.

City of New Orleans. 2019. Mirabeau Water Garden - Drainage Improvements and Green Infrastructure Project - Fact Sheet.

Dasgupta, S., S. Lall, and D. Wheeler. 2022, January 5. Cutting global carbon emissions: where do cities stand? https://blogs.worldbank.org/sustainablecities/cutting-global-carbon-emissions-where-do-c ities-stand.

Dronova, I., M. Friedman, I. McRae, F. Kong, and H. Yin. 2018. Spatio-temporal non-uniformity of urban park greenness and thermal characteristics in a semi-arid region. Urban Forestry & Urban Greening 34:44–54.

Du, H., W. Cai, Y. Xu, Z. Wang, Y. Wang, and Y. Cai. 2017. Quantifying the cool island effects of urban green spaces using remote sensing Data. Urban Forestry & Urban Greening 27:24–31.

ESRI (Hong Kong). 2022, July 21. Hong Kong 18 Districts. Feature layer, ESRI.
Estimating the Land Surface Temperature (LST) using Landsat 8 in ArcGIS. 2021.

Hill, K. 2016. Climate Change: Implications for the Assumptions, Goals and Methods of Urban Environmental Planning. Urban Planning 1:103–113.

Hong Kong Observatory. 2021a. Annual mean temperature projection for Hong Kong. https://www.hko.gov.hk/en/climate_change/proj_hk_temp_mean.htm.

Hong Kong Observatory. 2021b. Monthly Means of Meteorological Elements for Hong Kong Observatory, 1991-2020. https://www.hko.gov.hk/en/cis/region_climat/mean.htm.

Hong Kong Observatory. 2021c. Monthly Means of Meteorological Elements for Tuen Mun, 1988-2021. https://www.hko.gov.hk/en/cis/region_climat/mean.htm.

Hong Kong SAR Government. 2021. Hong Kong's Climate Action Plan 2050:66. Hong Kong's Climate Action Plan 2050. 2021. :66.

IPCC. 2022. Summary for Policymakers. Pages 3–33. Cambridge, UK and New York, NY, USA.

Jaganmohan, M., S. Knapp, C. M. Buchmann, and N. Schwarz. 2016. The Bigger, the Better? The Influence of Urban Green Space Design on Cooling Effects for Residential Areas. Journal of Environmental Quality 45:134–145.

Jerome, G. 2017. Defining community-scale green infrastructure. Landscape Research 42:223–229.

Kim, D., and S.-K. Song. 2019. The Multifunctional Benefits of Green Infrastructure in Community Development: An Analytical Review Based on 447 Cases. Sustainability 11:3917.

Kong, F., H. Yin, P. James, L. R. Hutyra, and H. S. He. 2014. Effects of spatial pattern of greenspace on urban cooling in a large metropolitan area of eastern China. Landscape and Urban Planning 128:35–47.

Lai, C. 2017, February. Unopened Space: Mapping Equitable Availability of Open Space in Hong Kong. Civic Exchange.

Lakhani, N. 2022, October 25. Virtually all children on Earth will face more frequent heatwaves by 2050. The Guardian.

Lan, H., K. K.-L. Lau, Y. Shi, and C. Ren. 2021. Improved urban heat island mitigation using bioclimatic redevelopment along an urban waterfront at Victoria Dockside, Hong Kong. Sustainable Cities and Society 74:103172.

Laukkonen, J., P. K. Blanco, J. Lenhart, M. Keiner, B. Cavric, and C. Kinuthia-Njenga. 2009. Combining climate change adaptation and mitigation measures at the local level. Habitat International 33:287–292.

Lee, C. 2020, September 1. Hong Kong's public space problem. https://www.bbc.com/worklife/article/20200831-hong-kong-public-space-problem-social-distance.

Lennon, M., and M. Scott. 2014. Delivering ecosystems services via spatial planning: reviewing the possibilities and implications of a green infrastructure approach. The Town Planning Review 85:563–587.

Lin, P., S. S. Y. Lau, H. Qin, and Z. Gou. 2017. Effects of urban planning indicators on urban heat island: a case study of pocket parks in high-rise high-density environment. Landscape and Urban Planning 168:48–60.

Mabon, L., and W.-Y. Shih. 2018. What might 'just green enough' urban development mean in the context of climate change adaptation? The case of urban greenspace planning in Taipei Metropolis, Taiwan. World Development 107:224–238.

Maimaitiyiming, M., A. Ghulam, T. Tiyip, F. Pla, P. Latorre-Carmona, Ü. Halik, M. Sawut, and M. Caetano. 2014. Effects of green space spatial pattern on land surface temperature: Implications for sustainable urban planning and climate change adaptation. ISPRS Journal of Photogrammetry and Remote Sensing 89:59–66.

Makido, Y., D. Hellman, and V. Shandas. 2019. Nature-Based Designs to Mitigate Urban Heat: The Efficacy of Green Infrastructure Treatments in Portland, Oregon. Atmosphere 10:282.

Marando, F., M. P. Heris, G. Zulian, A. Udías, L. Mentaschi, N. Chrysoulakis, D. Parastatidis, and J. Maes. 2022. Urban heat island mitigation by green infrastructure in European Functional Urban Areas. Sustainable Cities and Society 77:103564.

Masoudi, M., and P. Y. Tan. 2019. Multi-year comparison of the effects of spatial pattern of urban green spaces on urban land surface temperature. Landscape and Urban Planning 184:44–58.

Meerow, S., and J. P. Newell. 2017. Spatial planning for multifunctional green infrastructure: Growing resilience in Detroit. Landscape and Urban Planning 159:62–75.

Ng, E., L. Chen, Y. Wang, and C. Yuan. 2012. A study on the cooling effects of greening in a high-density city: An experience from Hong Kong. Building and Environment 47:256–271.

Park, J., J.-H. Kim, D. K. Lee, C. Y. Park, and S. G. Jeong. 2017. The influence of small green space type and structure at the street level on urban heat island mitigation. Urban Forestry & Urban Greening 21:203–212.

Parker, J., and M. E. Zingoni de Baro. 2019. Green Infrastructure in the Urban Environment: A Systematic Quantitative Review. Sustainability 11:3182.

Peng, S., S. Piao, P. Ciais, P. Friedlingstein, C. Ottle, F.-M. Bréon, H. Nan, L. Zhou, and R. B. Myneni. 2012. Surface Urban Heat Island Across 419 Global Big Cities. Environmental Science & Technology 46:696–703.

Perini, K., and A. Magliocco. 2014. Effects of vegetation, urban density, building height, and atmospheric conditions on local temperatures and thermal comfort. Urban Forestry & Urban Greening 13:495–506.

Petralli, M., L. Massetti, G. Brandani, and S. Orlandini. 2014. Urban planning indicators: useful tools to measure the effect of urbanization and vegetation on summer air temperatures. International Journal of Climatology 34:1236–1244.

Razzaghi Asl, S., and H. Pearsall. 2022. How Do Different Modes of Governance Support Ecosystem Services/Disservices in Small-Scale Urban Green Infrastructure? A Systematic Review. Land 11:1247.

Resilience & Sustainability - Areas of Focus - Green Infrastructure - Hazard Mitigation - Stormwater Projects - Mirabeau Water Garden: Phase I. (n.d.). . https://nola.gov/resilience-sustainability/areas-of-focus/green-infrastructure/hazard-mitigation-stormwater-projects/mirabeau-water-garden-phase-i/.

Sturiale and Scuderi. 2019. The Role of Green Infrastructures in Urban Planning for Climate Change Adaptation. Climate 7:119.

Tan, Z., K. K.-L. Lau, and E. Ng. 2016. Urban tree design approaches for mitigating daytime urban heat island effects in a high-density urban environment. Energy and Buildings 114:265–274.

The Legislative Council Commission. 2021. Legislative Council of the Hong Kong Special Administrative Region - Measures to tackle urban heat. https://www.legco.gov.hk/research-publications/english/essentials-2021ise04-measures-to-tackle-urban-heat.htm.

Tuen Mun and Yuen Long West District Planning Office,Planning Department. 2019. Tuen Mun - Planning for Liveable New Towns.

Tuholske, C., K. Caylor, C. Funk, A. Verdin, S. Sweeney, K. Grace, P. Peterson, and T. Evans. 2021. Global urban population exposure to extreme heat. Proceedings of the National Academy of Sciences 118:e2024792118.

United Nations Children's Fund. 2022. The Coldest Year of the Rest of their Lives: Protecting children from the escalating impacts of heatwaves.

Urban Renewal Authority. (n.d.). The District Study for Yau Ma Tei and Mong Kok. https://www.ura.org.hk/en/major-studies-and-concepts/yau-tsim-mong-district-study.

U.S. Geological Survey. (n.d.). Landsat 9. https://www.usgs.gov/landsat-missions/landsat-9.

Vaz Monteiro, M., K. J. Doick, P. Handley, and A. Peace. 2016. The impact of greenspace size on the extent of local nocturnal air temperature cooling in London. Urban Forestry & Urban Greening 16:160–169.

Venditti, B. 2022, April 26. This chart shows the impact rising urbanization will have on the world. World Economic Forum.

World Health Organization. (n.d.). Heatwaves. https://www.who.int/health-topics/heatwaves.

Xiao, X., L. Zhang, Y. Xiong, J. Jiang, and A. Xu. 2022. Influence of spatial characteristics of green spaces on microclimate in Suzhou Industrial Park of China. Scientific Reports 12:9121.

Yau Tsim Mong District Council. 2015, June 4. Yau Tsim Mong District Council - District Highlights. https://www.districtcouncils.gov.hk/ytm/english/info/highlight_01.html.

Zhou, W., J. Wang, and M. L. Cadenasso. 2017. Effects of the spatial configuration of trees on urban heat mitigation: A comparative study. Remote Sensing of Environment 195:1–12.

Zielinski, S. 2014, July 9. Why the City Is (Usually) Hotter than the Countryside. https://www.smithsonianmag.com/science-nature/city-hotter-countryside-urban-heat-islan d-science-180951985/.

APPENDIX

Figure A1: Tuen Mun Landscape Network Metrics Single Variable Linear Regression

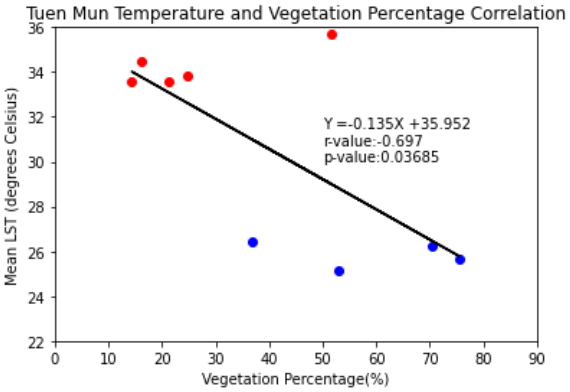

Figure A1a: Vegetation Percentage

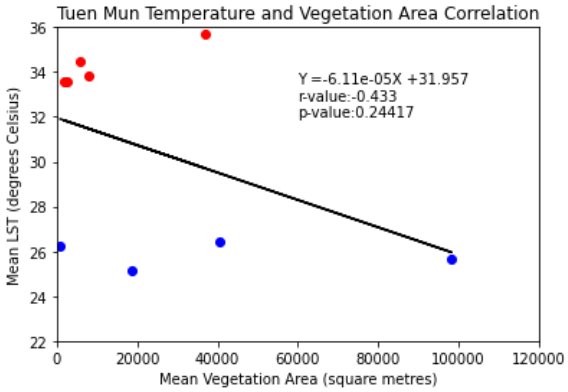

Figure A1b: Vegetation area

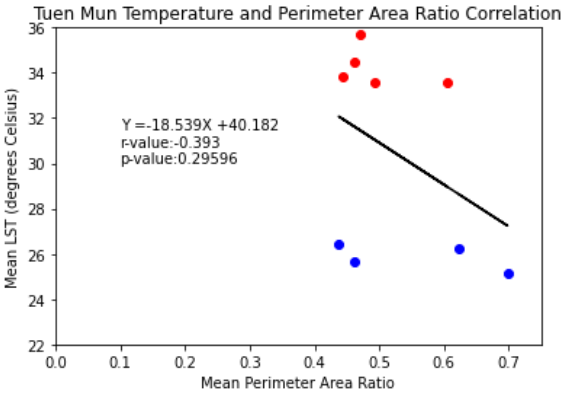

Figure A1c: Perimeter-area ratio

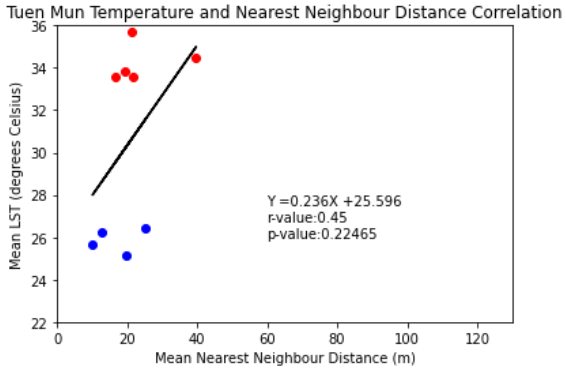

Figure A1d: Nearest neighbor distance

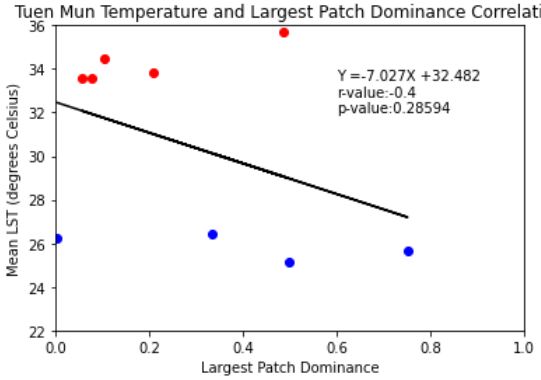

Figure A1e: Largest patch dominance

Figure A2: Yau Tsim Mong Landscape Network Metrics Single Variable Linear Regression

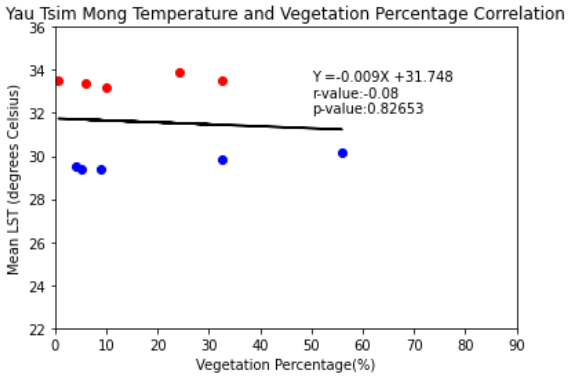

Figure A2a: Vegetation Percentage

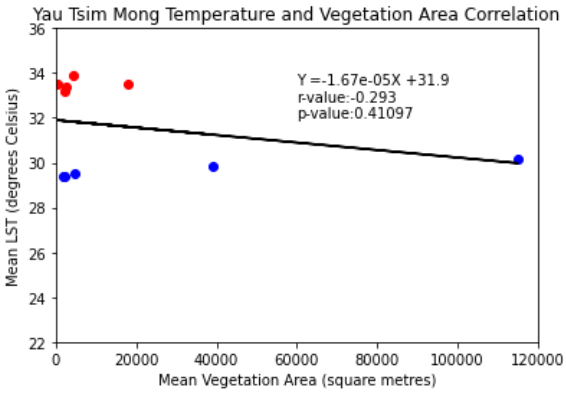

Figure A2b: Vegetation area

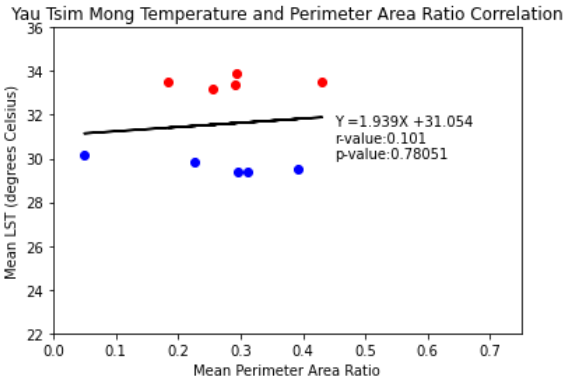

Figure A2c: Perimeter-area ratio

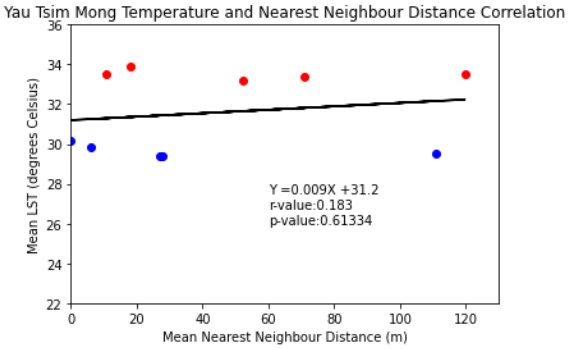

Figure A2d: Nearest neighbor distance

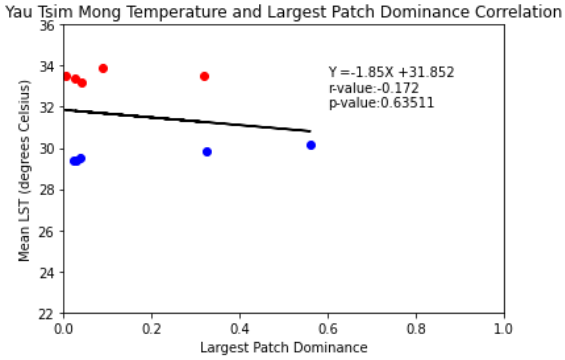

Figure A2e: Largest patch dominance

Figure A3: Hotspots (red) and Coldspot (blue) Landscape Network Metrics Single Variable Linear Regression

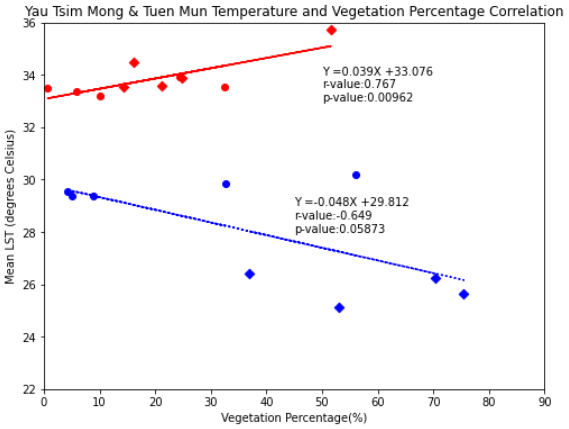

Figure A3a: Vegetation Percentage

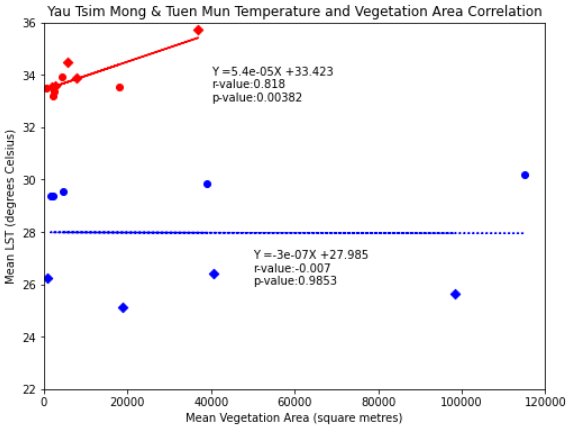

Figure A3b: Vegetation area

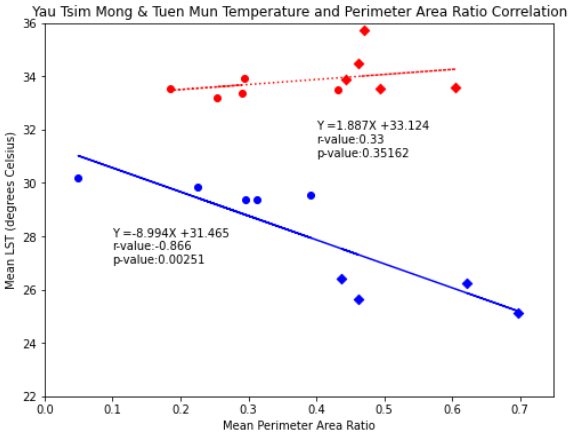

Figure A3c: Perimeter-area ratio

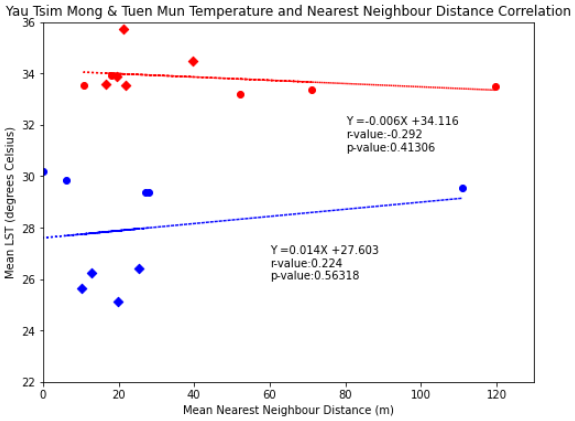

Figure A3d: Nearest neighbor distance

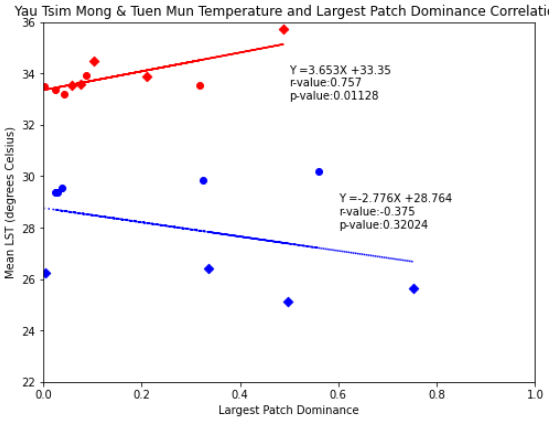

Figure A3e: Largest patch dominance

Table A1: Preliminary Multiple Linear Regression for Tuen Mun

R^2 value: 0.631		Prob (F-statistic): 0.526	
Landscape network metric	**P > |t|**	**Regression coefficient**	**Regression coefficient (normalized values)**
Vegetation percentage	0.584	-0.0746	
Vegetation area	0.455	-0.0001	
Perimeter-area ratio	0.360	-29.5034	
Nearest neighbor distance	0.723	-0.1015	
Largest patch dominance	0.580	9.6327	

Table A2: Preliminary Multiple Linear Regression for Yau Tsim Mong

R^2 value: 0.701		Prob (F-statistic): 0.281	
Landscape network metric	**P > |t|**	**Regression coefficient**	**Regression coefficient (normalized values)**
Vegetation percentage	0.096	0.3397	
Vegetation area	0.091	-0.0001	
Perimeter-area ratio	0.190	-25.1002	
Nearest neighbor distance	0.069	0.0727	
Largest patch dominance	0.303	-17.0317	

Table A3: Preliminary Multiple Linear Regression for Hotspots

R^2 value: 0.833		Prob (F-statistic): 0.102	
Landscape network metric	**P > |t|**	**Regression coefficient**	**Regression coefficient (normalized values)**
Vegetation percentage	0.557	0.0408	0.7993
Vegetation area	0.451	7.239×10^{-5}	1.0977
Perimeter-area ratio	0.257	1.6551	0.2895
Nearest neighbor distance	0.694	0.0053	0.2400
Largest patch dominance	0.469	-4.4885	-0.9299

Table A4: Preliminary Multiple Linear Regression for Coldspots

R^2 value: 0.989		Prob (F-statistic): 0.00376	
Landscape network metric	**P > |t|**	**Regression coefficient**	**Regression coefficient (normalized values)**
Vegetation percentage	0.066	0.0529	0.7095
Vegetation area	0.040	-18.6436	-1.5045
Perimeter-area ratio	0.007	-7.147×10^{-5}	-1.7961
Nearest neighbor distance	0.036	0.0268	0.4308
Largest patch dominance	0.121	4.2233	0.5704

Table A5: Refined Multiple Linear Regression for Tuen Mun

R^2 value: 0.578		Prob (F-statistic): 0.197	
Landscape network metric	**P > |t|**	**Regression coefficient**	**Regression coefficient (normalized values)**
Vegetation percentage	0.490	-0.0699	-0.3620
Vegetation area	0.502	-5.121×10^{-5}	-0.4275
Perimeter-area ratio	0.346	-20.1870	-0.3634

Table A6: Refined Multiple Linear Regression for Yau Tsim Mong

R^2 value: 0.088		Prob (F-statistic): 0.725	
Landscape network metric	**P > |t|**	**Regression coefficient**	**Regression coefficient (normalized values)**
Vegetation area	0.539	-1.534×10^{-5}	-0.2693
Nearest neighbor distance	0.912	0.0023	0.0476

Table A7: Refined Multiple Linear Regression for Hotspots

R^2 value: 0.795		Prob (F-statistic): 0.0174	
Landscape network metric	**P > |t|**	**Regression coefficient**	**Regression coefficient (normalized values)**
Vegetation area	0.005	5.621×10^{-5}	0.8523
Perimeter-area ratio	0.105	2.0244	0.3541
Nearest neighbor distance	0.752	0.0015	0.0669

Table A8: Refined Multiple Linear Regression for Coldspots

R^2 value: 0.945		Prob (F-statistic): 0.00859	
Landscape network metric	**P > |t|**	**Regression coefficient**	**Regression coefficient (normalized values)**
Vegetation percentage	0.765	-0.0052	-0.0699
Perimeter-area ratio	0.004	-9.0534	-0.8722
Nearest neighbor distance	0.452	0.0084	0.1355
Largest patch dominance	0.145	-2.2564	-0.3047